J|A|C|S
ARTICLES

Published on Web 10/13/2010

Ultrafast Multisequential Photochemistry of 5-Diazo Meldrum's Acid

Philipp Rudolf, Johannes Buback, Jochen Aulbach, Patrick Nuernberger, and Tobias Brixner*

Institut für Physikalische und Theoretische Chemie, Universität Würzburg, Am Hubland, 97074 Würzburg, Germany

Received March 26, 2010; E-mail: brixner@phys-chemie.uni-wuerzburg.de

Abstract: We disclose the light-induced dynamics and ultrafast formation of several photoproducts from the manifold of reaction pathways in the photochemistry of 5-diazo Meldrum's acid (DMA), a photoactive compound used in lithography, by femtosecond mid-infrared transient absorption spectroscopy covering several nanoseconds. After excitation of DMA dissolved in methanol to the second excited state S_2, 70% of excited molecules relax back to the S_0 ground state. In competing processes, they can undergo an intramolecular Wolff rearrangement to form ketene, which reacts with a solvent molecule to an enol intermediate and further to carboxylate ester, or they first relax to the DMA S_1 state, from where they can isomerize to a diazirine and via an intersystem crossing to a triplet carbene. For a reliable identification of the involved compounds, density functional theory calculations on the normal modes and Fourier transform infrared spectroscopy of the reactant and the photoproducts in the chemical equilibrium accompany the analysis of the transient spectra. Additional experiments in ethanol and 2-propanol lead to slight spectral shifts as well as elongated time constants due to steric hindrance in transient spectra connected with the ester formation channel, further substantiating the assignment of the occurring reaction pathways and photoproducts.

Introduction

In photolithography α-diazocarbonyls play an essential role in electronic microchip production and many other industrial chemistry procedures.[1,2] The key properties making them so useful as photoactive compounds in positive photoresists are based upon the photoinduced loss of a diazo group accompanied by a re-formation of the molecular structure to form ketene, also known as Wolff rearrangement,[3,4] whose mechanism has given rise to a long controversy. It can take place in a concerted manner, where the ketene is formed directly by losing the diazo group synchronously with the rearrangement, or a stepwise one, where the ketene is formed via a carbene intermediate and a subsequent rearrangement, or a concurrent combination of both.[5−8] By using ultrafast transient absorption spectroscopy, intermittent reaction dynamics become observable and evidence for different reaction schemes has been collected, as recently reviewed by Burdzinski and Platz.[9] It was even reckoned that all cyclic diazocarbonyl compounds exhibit a dominant concerted and a minor stepwise reaction pathway.

This assumption is in line with our recent ultrafast study of diazonaphthoquinone, widely used for photoresist applications,[2] in which we found a formation of the ketene within 300 fs or faster, proving a concerted mechanism, but also indications for a concurrent carbene formation.[10,11] Blancafort and co-workers confirmed computationally that such a stepwise mechanism should be possible as well for this molecular system.[12] In an experiment on 5-diazo Meldrum's acid (DMA), Burdzinski et al.[13] observed a subpicosecond ketene formation, i.e., a concerted mechanism, but also contributions assigned to a singlet carbene with a lifetime of only 2.3 ps.

However, although DMA exhibits a rich photochemistry, ultrafast studies[13−15] have not addressed successive reaction dynamics of the ketene and carbene species and the information this can provide about intermediate products. This also is of interest with regard to DMA applications, since DMA is employed for high-resolution purposes as a photoactive com-

(1) Ito, H. Deep UV resist systems. In *Radiation Curing in Polymer Science and Technology IV: Practical Aspects and Applications*; Fouassier, J. P., Rabek, J. F., Eds.; Elsevier: London, 1993.
(2) Hacker, N. P. Photoresists and their development. In *Processes in Photoreactive Polymers*; Krongauz, V. V., Trifunac, A. D., Eds.; Chapman & Hall: New York, 1995.
(3) Nikolaev, V. A.; Khimich, N. N.; Korobitsyna, I. K. *Chem. Heterocycl. Compd.* **1985**, *21*, 264.
(4) Kirmse, W. *Eur. J. Org. Chem.* **2002**, *2002*, 2193.
(5) Popik, V. V. *Can. J. Chem.* **2005**, *83*, 1382.
(6) Wang, Y.; Yuzawa, T.; Hamaguchi, H.; Toscano, J. P. *J. Am. Chem. Soc.* **1999**, *121*, 2875.
(7) Burdzinski, G. T.; Wang, J.; Gustafson, T. L.; Platz, M. S. *J. Am. Chem. Soc.* **2008**, *130*, 3746.
(8) Bogdanova, A.; Popik, V. V. *J. Am. Chem. Soc.* **2004**, *126*, 11293.
(9) Burdzinski, G.; Platz, M. S. *J. Phys. Org. Chem.* **2010**, *23*, 308.
(10) Wolpert, D.; Schade, M.; Brixner, T. *J. Chem. Phys.* **2008**, *129*, 094504.
(11) Wolpert, D.; Schade, M.; Langhojer, F.; Gerber, G.; Brixner, T. *J. Phys. B* **2008**, *41*, 074025.
(12) Li, Q.; Migani, A.; Blancafort, L. *J. Phys. Chem. A* **2009**, *113*, 9413.
(13) Burdzinski, G.; Rehault, J.; Wang, J.; Platz, M. S. *J. Phys. Chem. A* **2008**, *112*, 10108.
(14) Lippert, T.; Koskelo, A.; Stoutland, P. O. *J. Am. Chem. Soc.* **1996**, *118*, 1551.
(15) Lippert, T.; Stoutland, P. O. *Appl. Surf. Sci.* **1997**, *109−110*, 43.

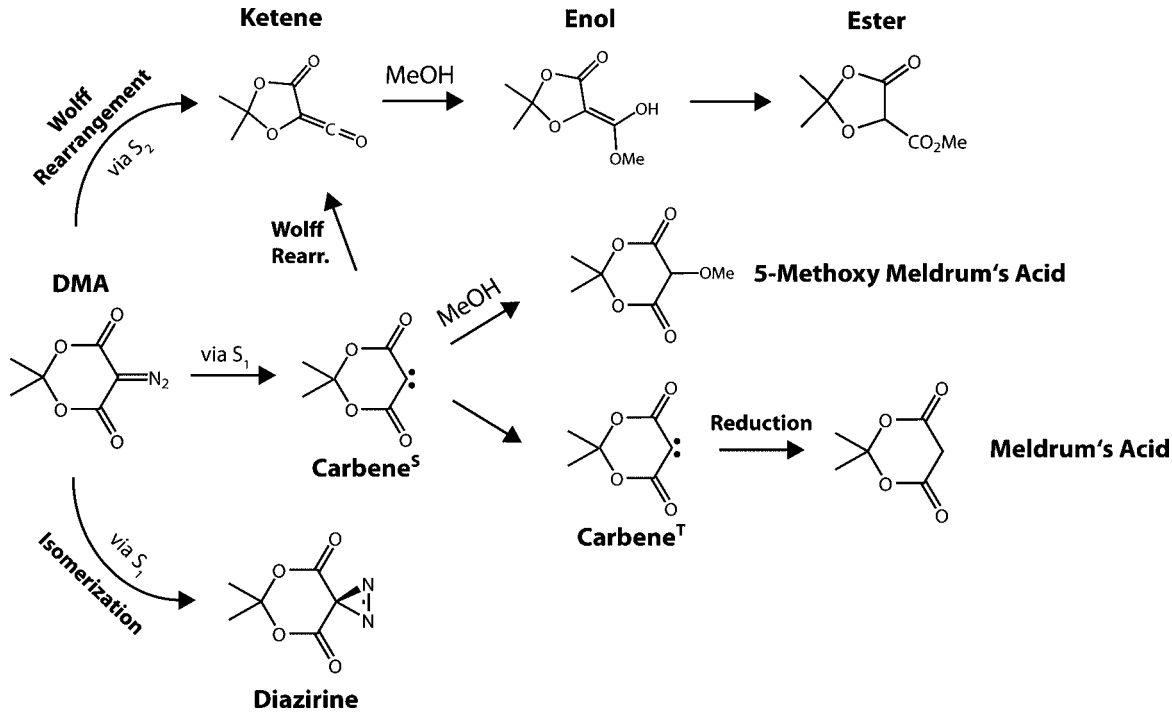

Figure 1. Scheme of the photoreaction of DMA dissolved in methanol. DMA in conjunction with an R−OH solvent provides three main reaction channels upon photoexcitation: (1) Wolff rearrangement reaction that forms ketene and ends up in an ester formation, (2) carbene formation that leads to Meldrum's acid by reducing the triplet carbene molecule, (3) isomerization of the DMA molecules to diazirine. Adapted from ref 23. Copyright 2003 American Chemical Society.

pound in deep ultraviolet (UV) lithography[1,2,16,17] and as a dopant for laser ablation in polymer matrixes.[14,15,18−20] Known reactions after excitation with UV light comprise the formation of a carboxylate ester via an intramolecular Wolff rearrangement; further reaction channels are an isomerization to diazirino Meldrum's acid and a reduction to Meldrum's acid,[21−24] as illustrated in Figure 1.

In this work, we unravel the first nanoseconds of the multisequential photoreaction dynamics of DMA, revealing ultrafast structural dynamics, characteristic time scales, and associated emerging chemical species. We focus on the light-induced bimolecular reaction in alcohol solution, where a reaction with a solvent molecule can occur for both the ketene and the carbene species accessible after UV excitation. These bimolecular reactions also provide a contribution to the question of whether and under which condition both ketene and carbene are formed for a specific compound, since subsequent reaction paths to distinct photoproducts are present which can be identified by their absorption characteristics. To reliably identify the reaction products, the transient spectra are complemented by density functional theory (DFT) calculations on the normal modes and Fourier transform infrared (FTIR) spectroscopy of both the reactant and the products in the chemical equilibrium, thus permitting a coherent picture of the ultrafast photochemistry of DMA.

Materials and Methods

The femtosecond pump−probe setup employed for the time-resolved experiments is based on a titanium:sapphire (Ti:Sa) chirped pulse amplification laser system, delivering pulses with a duration of 80 fs and energy of up to 1 mJ at a center wavelength of 800 nm and a repetition rate of 1 kHz. A fraction of the pulse energy was frequency doubled in a 300 μm β-barium borate (BBO) crystal to generate 400 nm pulses with pulse energies of up to 50 μJ. In a following sum-frequency generation process, the remaining 800 nm pulses were mixed with the 400 nm pulses in a 200 μm BBO crystal to create 266 nm pump pulses with pulse energies of up to 12 μJ (measurements in the 2000−2250 cm^{-1} wavenumber range were carried out with a 4 μJ pump pulse energy). The spot diameter at the place of the sample was adjusted to 350 μm. Tunable mid-infrared probe pulses were generated by parametric processes. A home-built two-stage optical parametric amplifier (OPA) similar to the design in ref 25 is pumped by the Ti:Sa fundamental pulses (300 μJ). The OPA generates tunable signal and idler pulses. Subsequent difference frequency mixing in a 1 mm thick $AgGaS_2$ crystal yields mid-infrared pulses with a spectral width of about 160 cm^{-1}. For the experiments in this work they were tuned between 1550 and 2250 cm^{-1}.

The probe pulses were focused into the sample to a spot diameter of 260 μm, and the energy at the sample position was 350 nJ. The polarizations of the pump and probe beams were set to the magic angle configuration of 54.7°. A time resolution of 350 fs could be achieved, as determined by observing the mid-infrared absorption rise in a thin germanium window following photoexcitation by the 266 nm pump pulse. After passing through the sample, the mid-

(16) Grant, B. D.; Clecak, N. J.; Twieg, R. J.; Willson, C. G. *IEEE Trans. Electron Devices* **1981**, *28*, 1300.
(17) Endo, M.; Tani, Y.; Sasago, M.; Nomura, N.; Das, S. *Jpn. J. Appl. Phys., Part 1* **1989**, *28*, 2357.
(18) Winnik, M. A.; Wang, F.; Nivaggioli, T.; Hruska, Z. *J. Am. Chem. Soc.* **1991**, *113*, 9702.
(19) Fujiwara, H.; Nakajima, Y.; Fukumura, H.; Masuhara, H. *J. Phys. Chem.* **1995**, *99*, 11481.
(20) Hahn, C.; Lippert, T.; Wokaun, A. *J. Phys. Chem. B* **1999**, *103*, 1287.
(21) Shevchenko, V. V.; Khimich, N. N.; Platz, M. S.; Nikolaev, V. A. *Russ. J. Org. Chem.* **2006**, *42*, 1213.
(22) Nikolaev, V. A.; Shevchenko, V. V.; Platz, M. S.; Khimich, N. N. *Russ. J. Org. Chem.* **2006**, *42*, 815.
(23) Bogdanova, A.; Popik, V. V. *J. Am. Chem. Soc.* **2003**, *125*, 14153.
(24) Bogdanova, A.; Popik, V. V. *J. Am. Chem. Soc.* **2003**, *125*, 1456.
(25) Hamm, P.; Kaindl, R. A.; Stenger, J. *Opt. Lett.* **2000**, *25*, 1798.

infrared probe pulses were sent to a spectrograph (Chromex 250 is/sm spectrograph/monochromator), where they were dispersed by a 150 lines/mm grating. They were detected by a 32-element mercury cadmium telluride photoconductive detector array (Infrared Associates, Inc.) with a spectral resolution of 10.2 nm (equivalent to about 3−5 cm^{-1}/pixel, depending on the probe wavelength regime). The whole experimental setup is permanently purged with dry air to minimize absorption due to air humidity. A mechanical chopper operating at 500 Hz blocks every other pump pulse, and successive probe signals, with a constant background subtracted, were processed on a shot-to-shot basis to obtain the pump-induced change in the optical density (OD) of the sample. The detection sensitivity of this femtosecond spectrometer reaches values of $\Delta OD = 10^{-4}$.

The single kinetic traces were recorded by using a motorized 600 mm delay line, allowing a temporal delay of 3.5 ns between the pump and probe pulses. The step size was chosen smaller around the temporal overlap than at longer delay times (which is reflected in the density of data points in the transient data). We did not observe an effect of varying pump−probe overlap for longer delay times due to misalignment or changes in the divergence of the pump beam, which in general would cause a continuous loss of signal, regardless of its sign or spectral position. The data analysis was performed with a sum of exponential functions.

The DMA sample was purchased from TCI Europe (CAS No. 7270-63-5) as 5-diazo-2,2-dimethyl-1,3-dioxane-4,6-dione. In all experiments it was used without further purification or other treatment and dissolved in spectroscopic-grade methanol, ethanol, or 2-propanol. Using a peristaltic pump, the sample circulated through a BaF_2 flow cell with an optical path length of 100 μm at a sufficiently high flow rate so that the sample volume is completely exchanged between successive laser shots. Due to the small extinction coefficient in the infrared, high sample concentrations of 47 mM were employed, leading to an optical density of 1.5 at 266 nm. Steady-state infrared spectra were recorded by a Fourier transform infrared (JASCO FT/IR-4100) spectrometer with a resolution of 1 cm^{-1}. Contributions of the solvent were taken into account by measuring the solvent spectrum separately and by subtracting it from the sample spectrum.

DFT calculations of DMA in vacuum were performed using the software package Gaussian 03.[26] In our calculations the density functional Becke three-parameter hybrid method[27,28] in combination with the Lee−Yang−Parr correlation functional (B3LYP)[29] was used. Both the molecular geometry optimization and the calculations for the normal modes and their amplitudes were carried out using the 6-311+G** basis set.

Results

DFT Calculations and FTIR Spectroscopy. FTIR spectra were recorded for DMA dissolved in methanol and initially without any previous photochemical conversion (Figure 2a, blue). The absorption spectrum in the chemical equilibrium shows significant bands at 1719, 1735, and 1753 cm^{-1} that can clearly be identified with combined stretching modes of C═O groups, while the strong absorption band at 2172 cm^{-1} should be assigned to the stretching vibration of the C═N═N group (compare, e.g., the value of 2169 cm^{-1} reported for this vibration for DMA in chloroform[9]). Other sample preparation techniques in the solid phase [attenuated total reflection (ATR) and DMA pressed in a KBr pellet] reproduced the absorption bands of the solution-phase spectra exactly. Furthermore, the output of the DFT calculations for DMA in methanol confirm the assignment of the occurring absorption bands and will be discussed in more detail later.

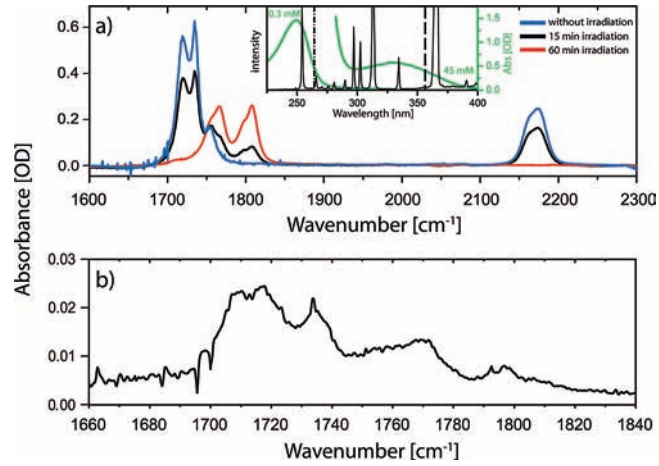

Figure 2. FTIR spectra of (a) a DMA/MeOH dissolution in the original state as well as after irradiation with a medium-pressure UV lamp and (b) a frequency-tripled pulsed Nd:YAG laser. The inset in (a) shows in green the UV/vis absorption spectrum of DMA (note the different concentrations to uncover the weaker absorption band at 330 nm) and the spectra of the medium-pressure UV lamp (black curve), the Nd:YAG laser (dashed line), and the UV excitation pulses (dotted−dashed line). (a) Blue curve: Under initial conditions mid-infrared steady-state absorption spectroscopy reveals four significant bands at 1719, 1735, and 1753 cm^{-1} (combined stretching modes of C═O groups) and at 2172 cm^{-1} (stretching vibration of the C═N═N group). After 15 min (black curve) and 60 min (red curve) of irradiation with a UV emitter, the DMA-specific absorption at 2172 cm^{-1} decreases toward zero while new maxima of absorption rise at 1766 and 1808 cm^{-1}. (b) After 10 min of irradiation with a frequency-tripled Nd:YAG laser, the same kind of diminishing DMA absorption can be noticed while new absorption bands at 1710, 1768, and 1796 cm^{-1} appear. Note the different *x*-axis scales.

In addition, two different radiation sources were applied to get a first impression of the photoproducts whose appearance should also be expected in the transient absorption experiments. According to UV/vis spectra (see the inset of Figure 2a), DMA exhibits a strong absorption signature in the UV regime around 245 nm and a minor one at 330 nm. Therefore, we used a medium-pressure UV radiation source with a broad but distinct line spectrum in the UV and visible spectral regions that provides high emission at 255 nm, while the emission bands beyond 300 nm only excite a few molecules due to the much weaker DMA absorption. The sample was positioned in a silica tube surrounded by the mentioned radiator. Figure 2a shows the FTIR spectra of DMA in methanol after 15 min (black) and 60 min (red) of such irradiation. By looking at the decreasing absorption band of the diazo group at 2172 cm^{-1}, one can state that after 15 min of irradiation nearly one-third of the DMA molecules have been converted and that after 1 h of irradiation the reactant has been converted completely. In the regime around 1740 cm^{-1} both of the primary maxima of absorption vanish while gradually new major absorption bands at 1766 and 1808 cm^{-1} and minor ones at 1760 and 1805 cm^{-1} rise. It has to be noted that these data do not show the pure excitation belonging to the 245 nm absorption band (because of the spectrally broad UV excitation), yet the aspired reaction channel with its intermediates will contribute significantly.

The second radiation source we used was a frequency-tripled pulsed Nd:YAG laser (355 nm, nanosecond pulse duration). Figure 2b shows the FTIR spectrum of DMA in methanol after 10 min of such irradiation. Again ca. 30% of the educt has been

(26) Frisch, M. J.; et al. *Gaussian 03*; Gaussian, Inc.: Wallingford, CT, 2004.
(27) Becke, A. D. *Phys. Rev. A* **1988**, *38*, 3098.
(28) Becke, A. D. *J. Chem. Phys.* **1993**, *98*, 5648.
(29) Lee, C. T.; Yang, W. T.; Parr, R. G. *Phys. Rev. B* **1988**, *37*, 785.

converted, which leads to emerging absorption signatures at 1710, 1768, and 1796 cm^{-1}.

In combination with the FTIR data, we calculated the optimal molecular geometry and with it the vibrational normal modes in different environments (isolated, chloroform, methanol) of any chemical species that we expected to find in the transient data as well. In terms of the upcoming time-resolved experiments, we concentrate here on the methanol solvent and find—besides a slight shift due to the solvent—very good agreement concerning the spectral positions with the calculations of Burdzinski et al.[13] The chemical species of interest are in general the emerging products and intermediates of a thermal or photolytic conversion of α-diazocarbonyl compounds.[23]

The corresponding subsumption is sketched in Figure 3. Apart from the triple splitting of the reactant's C═O absorption, which could not be reproduced by the DFT calculations, there is good agreement between experiment and theory, although all theoretical results tend to be slightly higher wavenumbers in comparison to the FTIR outcomes. These deviations might be adjusted by applying an appropriate scaling factor for the DFT results,[30] but we refrained from introducing it due to a limited gain in information content for the upcoming analysis. While the DFT prediction for the diazo absorption and for the ketene C═C═O absorption should lie at lower wavenumbers,[14] the bands can be unambiguously identified and the exact wavenumber can be determined from the absorption spectra.

The strong modes at 2172 cm^{-1} and in the region around 1740 cm^{-1} belonging to the reactant absorption will be taken as marker modes for the transient absorption measurements (in the following identifiable as ground-state bleach), since these comprise characteristic spectral signatures to observe diazo as well as C═C═O keto group vibrations, and C═O stretching vibrations, respectively.

Femtosecond Mid-Infrared Spectroscopy. The photochemistry of DMA in methanol upon photoexcitation with frequency-tripled Ti:Sa pulses at a wavelength of 266 nm spans at least three distinguishable reaction channels, some of which are of the bimolecular kind (see Figure 1). Femtosecond vibrational spectroscopy was applied in the spectral regions from 1550 to 1900 cm^{-1} and from 2000 to 2250 cm^{-1}, whereas only data are shown that actually illustrate any kind of transient absorption signal.

Figure 4 gives an overview of the whole set of spectrally and time-resolved transient absorption signals of DMA dissolved in methanol. The colored two-dimensional contour plot on the right-hand side summarizes the transient spectral evolution of DMA around 2140 cm^{-1}, showing two important features: first, a negative change in absorbance centered at 2172 cm^{-1} that relaxes partially up to a level where it remains constant during the residual delay time and, second, a positive change in absorbance that increases in strength and shifts continuously from lower (2080 cm^{-1} right after the zero delay time) to higher wavenumbers until it remains steady at 2135 cm^{-1}. Within 500 ps, this positive absorption vanishes completely.

In more detail Figure 5 shows the related time evolution at chosen frequencies. In accordance with the steady-state spectra of DMA (see Figure 2), the negative absorption is assigned to the ground-state bleach (GSB) of DMA, more precisely to the bleaching of the C═N═N stretching vibration in the electronic ground state upon photoexcitation with a subsequent relaxation to the latter within 20 ps. From this bleach recovery, a quantum yield of 30% can be derived. In other words, 30% of the initially excited molecules do not relax back to the ground state but form further photoproducts.

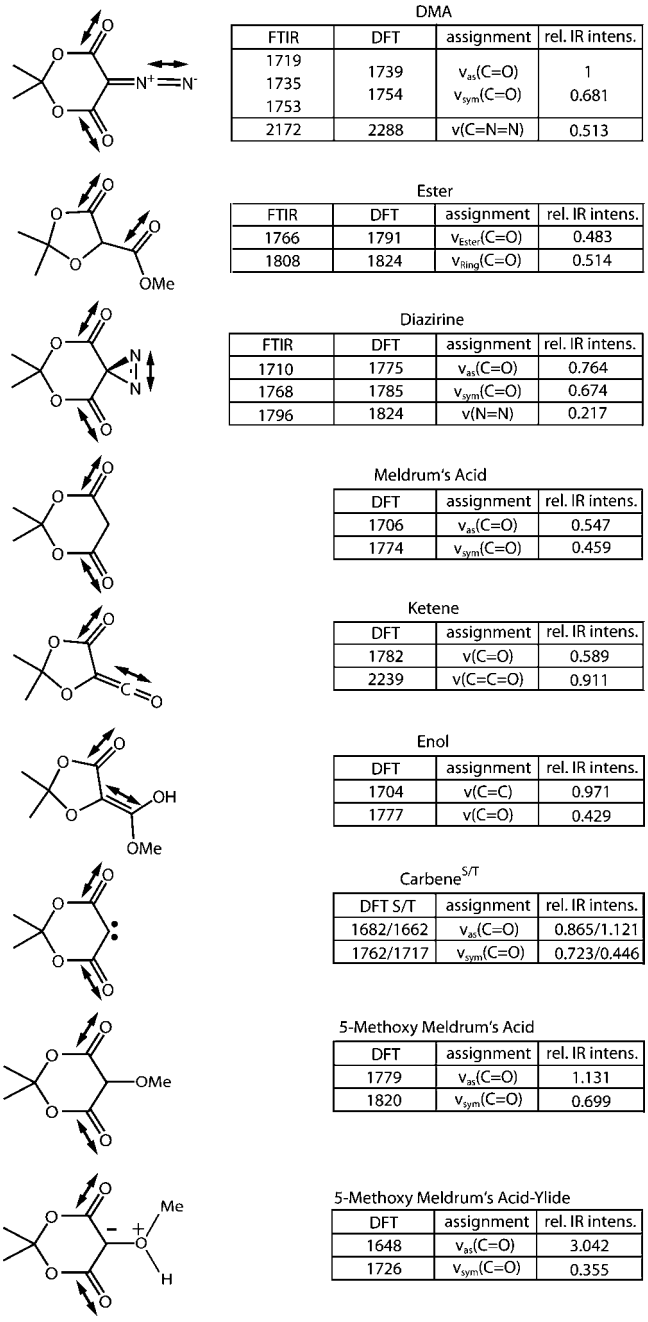

Figure 3. Illustration of the spectral position (cm^{-1}) of vibrational modes of the relevant chemical species in methanol, by DFT calculations on one hand and experimentally measured by FTIR spectroscopy on the other hand. As some species such as enol and ketene occur as intermediates, there are no FTIR data available. The amplitudes of the modes from the DFT calculations are given in the right-hand column, normalized to the strongest mode of DMA.

The positive absorption at 2135 cm^{-1} is assigned to the C═C═O stretching vibration of the ketene whose formation coincides with the DMA GSB. Its spectral position agrees very well with those in other studies,[13,14] and the behavior to shift toward higher frequencies within 15 ps can be explained by vibrational cooling of vibrationally excited ketene molecules.[31,32]

(30) Scott, A. P.; Radom, L. *J. Phys. Chem.* **1996**, *100*, 16502.

(31) Hamm, P.; Ohline, S. M.; Zinth, W. *J. Chem. Phys.* **1997**, *106*, 519.

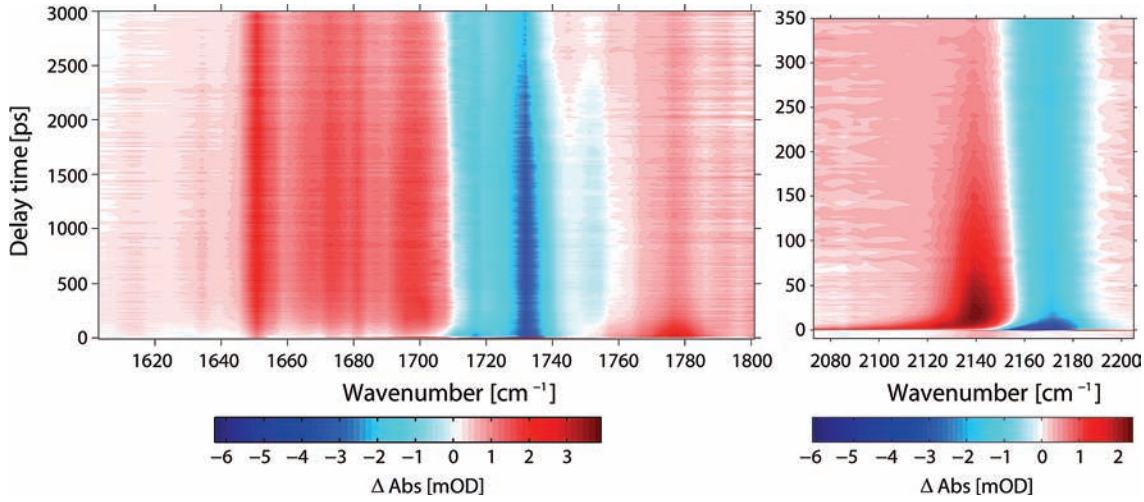

Figure 4. Colored two-dimensional contour plot of the temporally and spectrally resolved mid-infrared transient absorption experiments of DMA dissolved in methanol. In the regions both around 1740 cm^{-1} (absorption due to C═O stretching vibrations) and around 2170 cm^{-1} (absorption due to diazo and C═C═O keto stretching vibrations), one can see ground-state bleach of DMA after photoexcitation with 266 nm femtosecond pump pulses. Furthermore, a variety of significant positive contributions due to arising photoproducts illustrate the partly bimolecular photochemistry of DMA in methanol. Their origin and temporal progression are discussed by means of the particular transients (i.e., Figures 5−8).

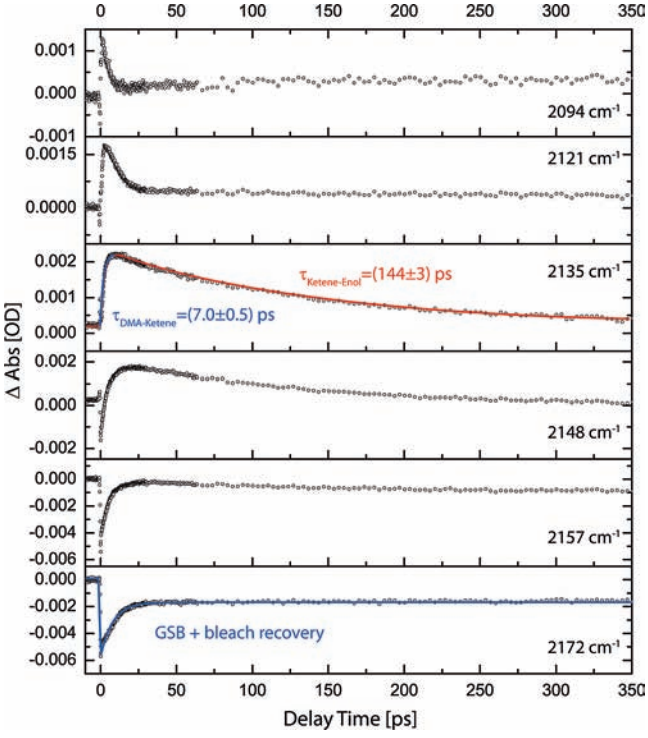

Figure 5. Exemplary transients from the spectral region between 2070 and 2200 cm^{-1} presenting the temporal evolution of (1) the GSB with a subsequent bleach recovery of DMA (2172 cm^{-1}), (2) the formation of the ketene intermediate that has an overall lifetime of 144 ps and is undetectable after roughly 500 ps (2135 cm^{-1}), and (3) the vibrational relaxation of "hot" ketene molecules (2080−2135 cm^{-1}).

Changes of absorption at negative delay times and the nearby zero delay time are due to the perturbed free induction decay (PFID) and the coherent artifact. From the former one can derive some information such as the line width of an absorption, but in general, it does not contain new information on molecular dynamics.[33−35] By contrast, absorption lines that only appear after the pump pulse do not exhibit a PFID, so that the rise times of the photoproducts reflect real dynamical information.[33,36] Measuring transient absorption spectra of pure methanol along the whole mentioned frequency domain did not show any dynamics.

On the left-hand side of Figure 4 one can see transient absorption signals between 1605 and 1805 cm^{-1}. Figure 6 gives a clearer insight into the temporal evolution of the particular transient absorption behavior that will be presented in the following. Reasons and explanations for the respective chemical assignments are given in the Discussion after the presentation of the experimental data.

It seems that these experimental results derive from various molecular dynamics. The most prominent and easily interpretable feature might be the broad negative contribution in the region around 1740 cm^{-1} that actually consists of three bands of absorption. It is assigned to the GSB of DMA molecules (detectable at this spectral position by characteristic C═O stretching vibrations) followed by the expected partial recovery (see Figure 6). Again the comparison of this spectral area with the steady-state spectra fits very well, as do the DFT calculations on the normal modes of DMA. An intrinsic physicochemical property of a transient describing a GSB is its constant level of absorption after the recovery. By contrast, the signal at 1732 cm^{-1} rises between 1500 and 3500 ps delay from a −4 to −1 mOD change in absorbance (see Figure 6). Also in the 1717 cm^{-1} transient this behavior is observed but less pronounced (from −1.5 to −1 mOD), indicating that a new absorption signal sets in which is blue-shifted relative to the GSB maximum at 1732 cm^{-1}. At 1740 cm^{-1} this new absorption leads to a change in sign of the transient absorption signal (from −1.1 to 0.3 mOD between 1500 and 3500 ps), while at 1757 cm^{-1} it can be observed in a mostly isolated fashion. At this spectral position there is only the weak tail of the ketene formation, together with a faint contribution of the DMA GSB during the first 3 ps, until from 1500 ps on a constant rise in absorbance occurs

(32) Laimgruber, S.; Schreier, W. J.; Schrader, T.; Koller, F.; Zinth, W.; Gilch, P. *Angew. Chem., Int. Ed.* **2005**, *44*, 7901.
(33) Hamm, P. *Chem. Phys.* **1995**, *200*, 415.
(34) Wynne, K.; Hochstrasser, R. M. *Chem. Phys.* **1995**, *193*, 211.
(35) Nuernberger, P.; Lee, K. F.; Bonvalet, A.; Polack, T.; Vos, M. H.; Alexandrou, A.; Joffre, M. *Opt. Lett.* **2009**, *34*, 3226.
(36) Nuernberger, P.; Lee, K. F.; Bonvalet, A.; Vos, M. H.; Joffre, M. *J. Phys. Chem. Lett.* **2010**, *1*, 2077.

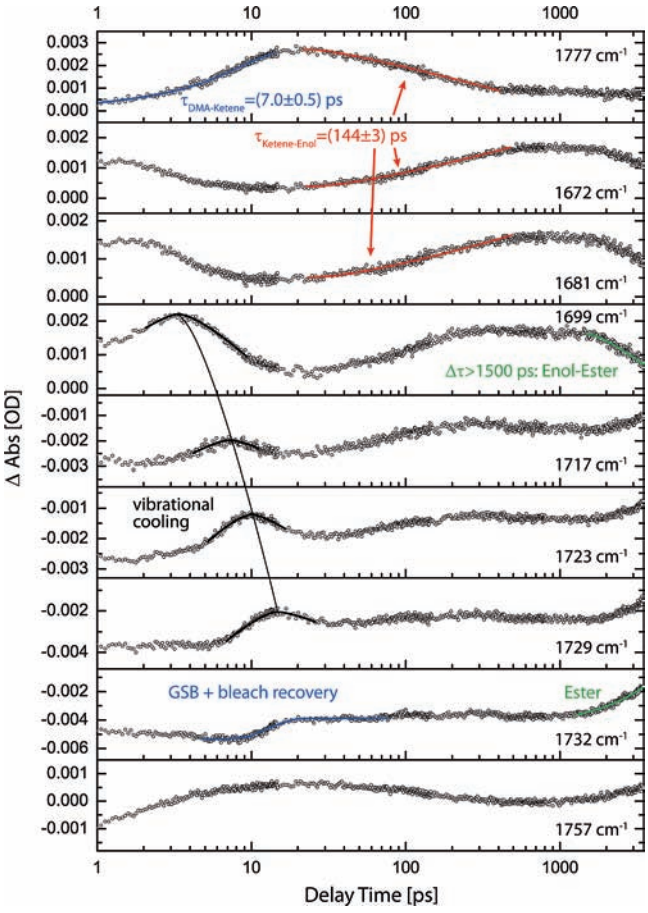

Figure 6. Characteristic transients from the spectral region between 1670 and 1780 cm^{-1} presenting the temporal evolution of (1) the GSB of DMA with the following bleach recovery, (2) the vibrational relaxation of excited DMA molecules in the electronic ground state, (3) the formation of the ketene intermediate arising from the absorption of C═O stretching vibrations, (4) its subsequent decrease due to the formation of a consecutive intermediate, and (5) again the decrease of the latter because of the emergence of a last measurable and consecutive photoproduct. The colored curves highlight the exponentially fitted regions of the transient data. Note the logarithmic time scale.

(from 0 to 0.5 mOD). This transient provides the same temporal development as the one at 1732 cm^{-1} but without the overlapping GSB. These characteristics cannot be found at any other position of the recorded time-resolved data.

For short delay times up to 20 ps in the spectral region beginning at 1655 cm^{-1} and fading into the GSB, one can observe once more a positive absorption that shifts with time toward higher intensities and frequencies, attributed to cooling of vibrationally "hot" DMA molecules in the S_0 ground state.[37,10] To specify, one can observe it in Figure 6 precisely during the first 20 ps in the transients at 1699, 1717, 1723, and 1729 cm^{-1}. Once the vibrational cooling process is completed, the ground-state bleach recovery reaches its highest level and remains constant.

Another transient absorption signal can be seen at 1777 cm^{-1}. Since it shows exactly the same temporal behavior after the zero delay time as the positive absorption at 2135 cm^{-1} (concerning both its formation and its decrease), this positive and short-living signal is assigned to the C═O stretching vibration of the arising ketene molecules. This attribution is perfectly confirmed by the DFT data (see Figure 3).

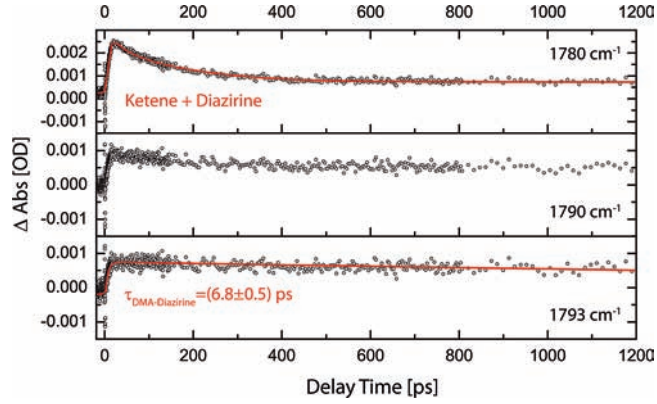

Figure 7. Transient of two superposed positive contributions of absorption (at 1786 cm^{-1}) deriving from the ketene formation and another photoproduct (at the top). The isolated temporal evolution of the latter is observable at the spectral position around 1793 cm^{-1}.

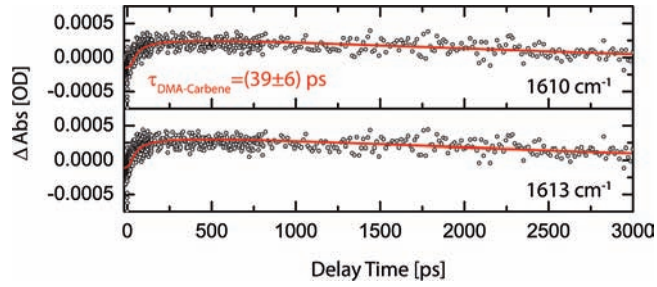

Figure 8. Transients describing a very weak absorption signal at 1613 cm^{-1}, whose temporal properties do not match any other recorded transient feature. It is therefore likely to constitute an independent signal associated with a molecular species not represented in the other signals.

In the spectral domain between 1635 and 1702 cm^{-1}, a broad contribution of positive absorbance occurs. It is composed of five specifiable kinetic traces whose intensity varies between ΔOD values of 0.5 and 2.3 mOD. All five traces exhibit an equal temporal behavior: They rise from the zero delay time on until they reach a maximum in absorbance after roughly 500 ps. The following plateau declines again for delays beyond 1500 ps and probably tends to a zero change of absorption after approximately 4 ns, although the latter cannot be detected due to the limited range of the employed delay stage. Figure 6 shows three transients (1672, 1681, and 1699 cm^{-1}) as an example of this temporal progression.

There is an interesting attribute about the transient signal at 1777 cm^{-1}: While the pure ketene absorption observable at 2135 cm^{-1} fully decreases toward 0 mOD within 500 ps (see Figure 5), this absorption does not. There is another underlying absorption signature which also shows up in an isolated fashion at 1793 cm^{-1} (see Figure 7). In comparison, their temporal evolution properties differ significantly for both short and long delay time scales.

Finally, at 1613 cm^{-1} a transient absorption signal was detected whose properties relating to its temporal development differ significantly from any other mentioned transient feature. Concerning the maximal change of absorption, it is the weakest signal of all recorded data with roughly 0.3 mOD. Figure 8 gives an overview of the according temporal evolution.

Influence of the Molecular Environment. On the basis of the fact that DMA dissolved in methanol provides different reaction channels upon photoexcitation (see ref 23), some of which include solvent molecules in the reaction dynamics while others

(37) Rini, M.; Holm, A.-K.; Nibbering, E. T. J.; Fidder, H. *J. Am. Chem. Soc.* **2003**, *125*, 3028.

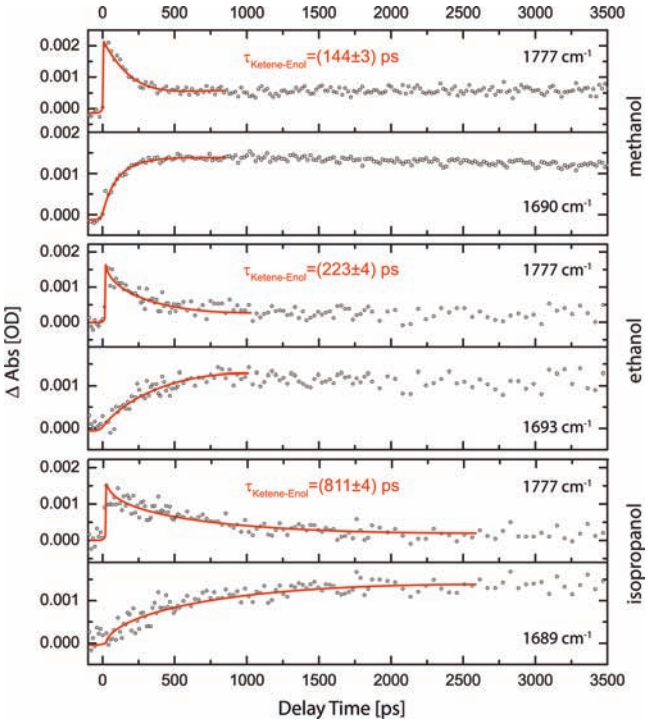

Figure 9. Representative transients regarding the steric hindrance of the photoreaction due to the molecular environment. Illustrated are transients of the ketene formation with its subsequent decomposition (around 1777 cm^{-1}) in conjunction with transients showing a simultaneous and temporally matching formation of a secondary product (depicted from the spectral region around 1690 cm^{-1}). In each case for methanol, ethanol, and 2-propanol as solvent, one can state that there is a consistent elongation of the time constants describing the photoreaction with increasing solvent viscosity.

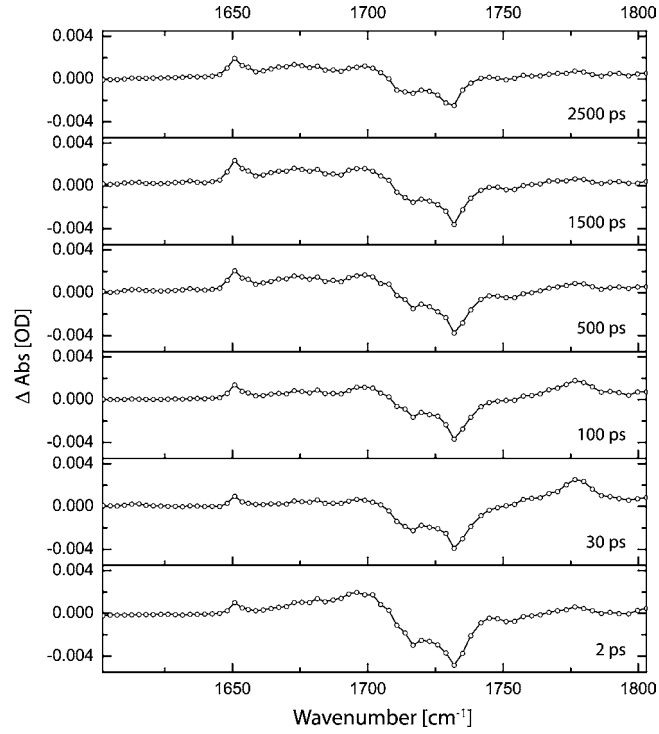

Figure 10. Transient mid-infrared spectra of DMA dissolved in methanol at different delay times between 2 and 2500 ps in the spectral region from 1605 to 1805 cm^{-1} illustrating on one hand the ground-state bleach of DMA. The positive changes of absorption on the other hand are discussed in more detail on the basis of the transients in Figures 6−8.

do not, we wanted to reveal which of the described transient features belong to what kind of reaction pathway. Therefore, additional time-resolved measurements were carried out with two solvents that exhibit a hydroxyl group as well, ethanol and 2-propanol, providing information on the steric hindrance of the photoreaction due to the molecular environment.

Figure 9 summarizes the main implications of the steric hindrance on the temporal evolution of the photoreaction. The results of these experiments are as follows: While the time constant of the ketene decomposition (detectable around 1777 and 2135 cm^{-1}) shifts significantly toward longer values with increasing solvent viscosity, the absorption band at 1793 cm^{-1} turns out to be nearly unaffected. Equally, the time constants describing the ketene formation, the GSB, and the bleach recovery do not change significantly by means of the molecular environment. In contrast to this, all the positive absorption signals between 1635 and 1702 cm^{-1} show a temporal elongation, in a simultaneous fashion for the respective solvent and temporally consistent with the decreasing ketene signatures. The steric hindrance also has an effect on the rise in absorbance at 1732 and 1757 cm^{-1} observed for delay times longer than 1500 ps in methanol. In the case of 2-propanol, it is retarded in such a way that it putatively sets in after the maximum delay time (i.e., 3.5 ns) and is therefore no longer detectable.

Discussion

We have to consider many different chemical species taking part in the investigated partly bimolecular reaction dynamics of DMA dissolved in methanol, ethanol, and 2-propanol. The DFT calculations already indicate overlapping or at least adjoining bands of absorption. The transient absorption spectra which were measured in two different spectral areas (from 1550 to 1900 cm^{-1} and between 2000 and 2250 cm^{-1}; see Figure 4) depict this circumstance. Figure 10 illustrates the discussed results in the spectral region between 1605 and 1805 cm^{-1} by means of plotted cuts along the frequency axis of Figure 4 at certain delay times. Via a sum of exponential fits, which provide time constants for the according molecular dynamics and which are complemented by additional analysis, steady-state spectra, and simulations, the entire set of transient absorption spectra are interpreted with the microscopic picture of the reaction in mind in the following way.

After excitation of the DMA molecule to the S_7 and S_5 states[13] and internal conversion to the S_2 state, nitrogen elimination occurs on a time scale too fast for our setup ($\tau \leq 350$ fs). This step is followed by a reaction involving a singlet carbene intermediate to the ketene. The [1,2]-shift of the alkoxide group seems to be the rate-determining step of this unimolecular reaction since no carbene intermediate can be detected. Between 2080 and 2140 cm^{-1}, one observes the vibrational cooling of vibrationally excited ketene molecules that reaches its final spectral position within 15 ps. At 2135 cm^{-1}, as well as at 1777 cm^{-1}, the formation of the ketene intermediate is observable with a time constant $\tau_{DMA-ketene} = 7.0 \pm 0.5$ ps (comparable to the transient absorption experiments on other diazocarbonyl compounds carried out by Vleggaar et al.[38]), whereas the nascent, vibrationally hot ketene molecules are formed within the time resolution of the transient spectrometer, in agreement with the recent studies of DMA in chloroform.[13] Due to this

(38) Vleggaar, J. J. M.; Huizer, A. H.; Kraakman, P. A.; Nijssen, W. P. M.; Visser, R. J.; Varma, C. A. G. O. *J. Am. Chem. Soc.* **1994**, *116*, 11754.

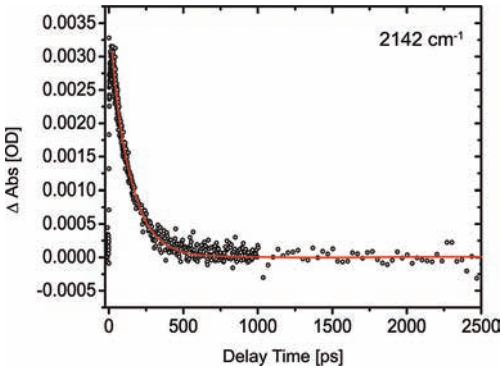

Figure 11. Transient at 2142 cm^{-1} demonstrating the complete decomposition of the ketene intermediate within 500 ps.

result, we can conclude that a concerted reaction clearly occurs, not excluding the appearance of a concurrent carbene formation, which yet supposedly manifests itself in a different spectral region (see below).

The ketene possesses a very electrophilic carbonyl atom in the ketene group, since it is part of a carbonyl group and part of a vinylogous carbonyl group (Michael system). The quasi-unimolecular kinetic of the nucleophilic addition of a methanol molecule to this carbon atom is therefore very fast with a time constant of $\tau_{ketene-enol} = 144 \pm 3$ ps. Since we suppose that the hard oxygen interacts preferably with the harder antibonding π^*-orbital of the carbonyl group instead of the softer π^*-orbital of the Michael system, the product of this addition reaction is the enol in Figure 12. The bleaching of the reactant (ketene) can be observed at the ketene mode at 2135 cm^{-1} and at its carbonyl mode at 1777 cm^{-1}, whereas the product formation (enol) can be followed at 1650−1700 cm^{-1}. The transients in Figure 6 underline the temporal consistency of this assignment. The Wolff rearrangement finishes with the keto−enol tautomerization, an intramolecular protonation−deprotonation step converting the enol into the ester. We suspect to see this process in our transient absorption data as well. In what follows for larger delays, it appears that the enol contributions decrease significantly after a 1500 ps delay time while at the same time a new absorption appears in the region around 1740 cm^{-1}. This superposition of the GSB and the rather late emergence of a photoproduct cannot be observed in other spectral regions, e.g., around 2170 cm^{-1}, where the isolated DMA GSB is recorded. We therefore assign this transient behavior to the tautomerization of the enol to the ester, the last link of the reaction channel that is initialized by the Wolff rearrangement. Figure 6 summarizes and illustrates this interpretation on the basis of characteristic transients.

The pure ketene absorption around 2135 cm^{-1} demonstrates that all contributions of the ketene vanish within the first 500 ps (see Figure 11) and consequently the change of absorption drops back to 0 mOD. The transient at 1777 cm^{-1} does not reproduce this result. From the zero delay time on the ketene absorption is superposed by a positive absorption that nearly remains constant along the whole time axis. This contribution is assigned to the formation of diazirine, which is practically stable on the time scale monitored here.[22] It emerges isolated at 1793 cm^{-1} with a time constant $\tau_{diazirine} = 6.8 \pm 0.5$ ps (see Figure 7). The DFT calculations predict an overlapping absorption of the ketene and the diazirine in good spectral agreement with the transient data.

Bogdanova et al.[23] state that the outcome of the photolysis of DMA is wavelength dependent in such a way that 355 nm irradiation should emphasize the formation of diazirine, as well as of Meldrum's acid, although the corresponding quantum efficiency stays quite low. Accordingly, Wolff rearrangement and isomerization derive from two different electronically excited states. (Zhang et al.[39] mention a minor photoinduced process leading *p*-methoxy-3-phenyl-3-methyldiazirine directly from the S_2 state to the corresponding diazo compound. Even if we assume a similar process taking place inversely, we cannot find indications in our data supporting this molecular behavior.) Our FTIR experiments (Figure 2) agree with this finding: The medium-pressure UV radiator produced mainly ester molecules and minor contributions of diazirine (due to the continuous radiation spectra). The referring FTIR data show new strong absorption bands at 1766 and 1808 cm^{-1} (ester assignment) and a weak one at 1796 cm^{-1}. The Nd:YAG laser should preferentially produce diazirine and suppress the ester formation. Consistently, the FTIR data do not show new absorption bands around 1740 and 1760 cm^{-1} but again at 1796 cm^{-1}. Meldrum's acid could also be produced in at most minor quantities, which is confirmed by Figure 2, where we find no pronounced peaks at its two absorption maxima (at 1753 and 1785 cm^{-1}).[40,41] Additionally, the FTIR measurements denote an absorption band around 1710 cm^{-1} that consequently derives from the lower electronically excited state too. However, since the quantum efficiency for this pathway is obviously quite low, it seems hardly feasible to separate this contribution from the strong positive enol absorption and the nearby lying similarly strong negative DMA GSB in the time-resolved data. Not only is Meldrum's acid formation expected to be marginal, but diazirine also better fits into the assignment of the steady-state and transient data when taking the overall upshift in frequency of the DFT calculations into account. Moreover, the similar rise time of the transients at 1777 and 1793 cm^{-1} underlines this identification since diazirine formation should occur on a time scale similar to that of ketene formation. The formation of Meldrum's acid would take longer, regardless of whether Meldrum's acid is a reaction product of a triplet carbene or of a singlet carbene species that interacts with solvent molecules by inserting an OH group and subsequently undergoing the Norrish type II phototransformation.[22] Hence, the identification of photoproducts in the transient and the FTIR data is in good agreement.

The experiments investigating the influence of the solvent on the photoreaction support the described connections between transient absorption data and designated reaction channels: the upshift of time constants due to the growing molecular size of the solvent significantly affects reaction pathways where the solvent is involved, namely, the proceeding of the ketene to the enol, whereby the ester formation consequently gets retarded as well (see Figure 9). Molecular processes that do not interact directly with the solvent molecules such as the DMA GSB around 1740 and 2170 cm^{-1}, the ketene composition, the vibrational cooling of the ketene (around 2110 cm^{-1}) and the DMA (around 1700 cm^{-1}), or the absorption we assign to the diazirine formation remain virtually unaffected by the steric hindrance. These are first-step processes directly after the DMA excitation.

(39) Zhang, Y.; Burdzinski, G.; Kubicki, J.; Vyas, S.; Hadad, C. M.; Sliwa, M.; Poizat, O.; Buntinx, G.; Platz, M. S. *J. Am. Chem. Soc.* **2009**, *131*, 13784.
(40) Abramovitch, R. A. *Can. J. Chem.* **1959**, *37*, 361.
(41) Ernstbrunner, E. E. *J. Mol. Struct.* **1973**, *16*, 499.

At 1613 cm^{-1} the weakest positive change of absorption occurs within $\tau = 39 \pm 6$ ps and decays almost completely within 3 ns (see Figure 8). Possible intermediate precursors have a decay time of 39 ps or maybe even much shorter, with vibrational cooling and conformational changes possibly being responsible for the 39 ps rise of the observed species. These characteristics do not fit in with any other recorded and analyzed reaction channel (i.e., the Wolff rearrangement reaction with its subsequent photoproducts and the diazirine isomerization). Hence, it is possibly a signature of a triplet carbene to form Meldrum's acid. The very low signal intensity points at a low quantum efficiency for this reaction channel, which might indicate this cautious assignment, for which the excited system has to undergo an internal conversion and a subsequent intersystem crossing to enter this reaction pathway. Another assignment might be the 5-methoxy Meldrum's acid ylide.[44] The results from the DFT calculations in Figure 3 are in line with both assignments. On one hand, the calculated vibrational modes (1662 and 1644 cm^{-1}) are closer to 1613 cm^{-1} than any other mode of all the possible reaction intermediates and products, with the deviation actually being not too far if one takes into account the general trend that the vibrational frequencies are overestimated. On the other hand, we expect only small quantities of both species (triplet carbene and 5-methoxy Meldrum's acid ylide), but since the corresponding modes are in addition the strongest ones of all modes in Figure 3, an observation is not unlikely.

Following this hypothesis, the composition and decomposition of the singlet carbene should be completely carried out within 39 ps, although there is no direct evidence for it in our transient data. Other groups describing the temporal evolution of various carbene species under the very crucial impact of different solvents state lifetimes of similar magnitude.[42−44] More precisely, the singlet carbene of methyl styryldiazoacetate dissolved in methanol decays within 38 ps, while the triplet state persists on a time scale of some nanoseconds.[43] Other investigations with further chemical compounds such as *p*-biphenyl diazo species discovered upper lifetimes of the singlet carbene in the range of 700 ps.[7] However, Burdzinski et al. measured the lifetime of singlet carbene to be 2.3 ps (with DMA dissolved in chloroform). We can exclude that our observed signal originates from contaminations in the solvent (e.g., of water dissolved in methanol, which has an absorption band in this spectral region[45]), because we see no signal if only methanol is used. Considering these facts, an assignment of this transient to the triplet carbene or 5-methoxy Meldrum's acid ylide is likely but without having detected the previous singlet species or evidence for the subsequently formed Meldrum's acid/5-methoxy Meldrum's acid. An assignment to the singlet carbene does not seem reasonable due to the slow 39 ps rise time. This assignment merits further investigation in future studies.

The low quantum yield of the discussed transient in combination with the fact that there is neither a hint for a subsequent reaction channel in our transient data nor some indirect evidence in the transients describing the ketene dynamics makes a definite assignment of a molecular process corresponding to this spectral signature impossible. Hence, we find no evidence for a contribution of a stepwise Wolff rearrangement via a carbene intermediate in the transient data.

In the long term this absorption at 1613 cm^{-1} decreases monotonously with a time constant well beyond our maximum observation window. Likewise, the transients describing the diazirine development do too. This can be explained by a reisomerization of the diazirine to DMA. Unfortunately, due to the weakness of the according signals and the long decay time, this reisomerization of DMA could not be inferred from the GSB.

While we have disclosed the bimolecular reaction of the ketene intermediate on an ultrafast time scale, the fate of the carbene intermediate has to be further explored in future experiments to allow an unequivocal assignment.

Conclusions

Upon photoexcitation with 266 nm pump pulses, DMA is excited to a set of highly excited states (preferentially to the S_7 and S_5 states).[13] Within less than 100 fs the relaxation to the dissociative S_2 state takes place, from which the ketene formation following the Wolff rearrangement is initiated. Figure 12 gives an overview of the discussed experimental observations. Whereas the formation of diazirine and ketene occurs almost instantaneously after DMA excitation[9] and also ultrafast geminate recombination after N_2 cleavage cannot be excluded, the time constants given in Figure 12 represent how long it takes until these species are observable in the experiment. Vibrationally excited ketene molecules are formed via a very fast concerted mechanism. The according quantum efficiency amounts to 30% and therefore represents the highest developed reaction channel in these experiments. Subsequently, enol is formed by nucleophilic addition of the solvent (methanol, ethanol, or 2-propanol) to the ketene. Due to steric hindrance the temporal evolution of this process is strongly coupled to the involved solvent. After 1500 ps, the corresponding absorption bands begin to decrease while in the region of the DMA ground-state bleach (1740 cm^{-1}) a positive change of absorption begins to evolve (in comparison, the isolated DMA GSB that can be seen at 2172 cm^{-1} remains constant along the complete time axis). Under considerations of the temporal consistency and supporting analytical methods (i.e., DFT calculations and FTIR spectroscopy), this positive change of absorption is assigned to the ester. The ester represents the final step of the reaction channel that is initialized by the Wolff rearrangement.

In the course of the second possible reaction pathway, DMA relaxes to the first electronically excited state and isomerizes to form diazirine. This process appears in the transient spectra at 1777 and 1793 cm^{-1}. It is not affected by the solvent, which seems plausible since there is no solvent molecule involved in the isomerization process. Compared to the ketene formation, it exhibits a different temporal behavior concerning both the formation itself and the persistence on nanosecond time scales. A small absorption decrease can be explained by the reisomerization of the diazirine back to the DMA.

The transient data also revealed the existence of a weak spectrotemporal signature at 1613 cm^{-1} whose temporal properties differ from those of all other reaction channels and their absorption characteristics. Therefore, it is likely that it is associated with a further intermediate molecular species from the accessible reaction pathways, supposedly a triplet carbene involved in the reaction pathway toward the formation of

(42) Wang, J.; Kubicki, J.; Peng, H.; Platz, M. S. *J. Am. Chem. Soc.* **2008**, *130*, 6604.
(43) Zhang, Y.; Kubicki, J.; Platz, M. S. *J. Am. Chem. Soc.* **2009**, *131*, 13602.
(44) Wang, J.; Kubicki, J.; Gustafson, T. L.; Platz, M. S. *J. Am. Chem. Soc.* **2008**, *130*, 2304.
(45) Williams, D.; Gatica, T.; Gordy, W. *J. Phys. Chem.* **1937**, *41*, 645.

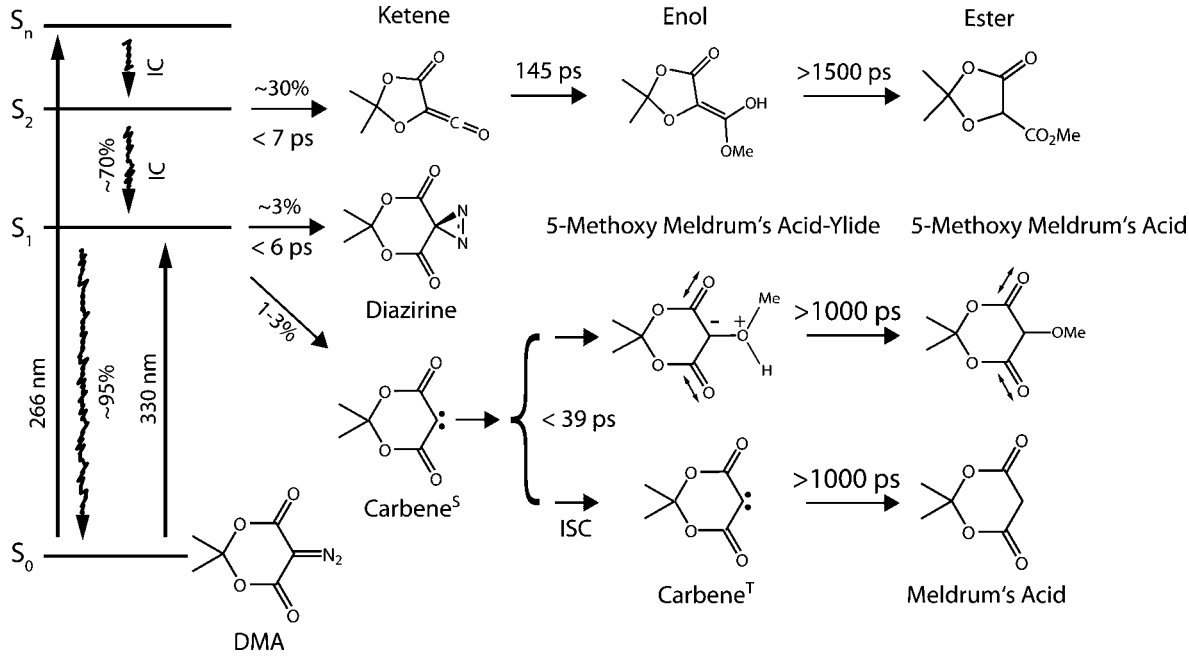

Figure 12. Schematic illustration of the detected reaction processes of DMA in methanol upon UV photoexcitation combined with the according experimentally investigated time constants. IC stands for internal conversion and ISC for intersystem crossing. The brace indicates two possible reaction pathways, both of which, according to the theoretical results, might explain the observed dynamics.

Meldrum's acid or a 5-methoxy Meldrum's acid ylide, deriving from the singlet carbene as well, which might evolve to form 5-methoxy Meldrum's acid.

The present work shows that time- and wavenumber-resolved experiments supported by calculations provide insight into complex processes, such as the photoreaction of DMA, which has parallel reaction pathways with multiple intermediate states. Whereas ketene formation from Wolff rearrangement has been observed on ultrafast time scales before, we also monitored the subsequent reaction in methanol solution from ketene to enol and further to ester, revealing that the complete reaction occurs on nanosecond time scales. The ultrafast photochemistry of DMA can serve as a prototype example for a multistep consecutive reaction, unraveled by the benefits of femtosecond mid-infrared spectroscopy.

Acknowledgment. We are grateful to Dr. Daniel Wolpert for his help in establishing parts of the experimental setup, to Matthias Parthey and Manuel Renz for their help concerning theoretical questions, and to Andreas Reuss for help with the Table of Contents figure. J.B. acknowledges financial support from the Fonds der Chemischen Industrie.

Supporting Information Available: Complete ref 26. This material is available free of charge via the Internet at http://pubs.acs.org/.

JA1025529